Elastic Tube Model Predictive Control With Scaled Zonotopic Sets

Sabin Diaconescu, Florin Stoican, *Member, IEEE*, Bogdan D. Ciubotaru, and Sorin Olaru, *Senior Member, IEEE*

***Abstract*—A novel parameterization of the tube associated with the Robust Model Predictive Control law is proposed. The aim is to reduce the computational complexity by describing the tube as a sequence of elastically-scaled zonotopic sets. The developments demonstrate the efficacy within the context of constrained control of a system affected by additive and bounded exogenous disturbances. The underlying set containment conditions using zonotopic sets result in linear complexity.**

***Index Terms*—Constrained control, predictive control for linear systems, robust control.**

I. Introduction

Model predictive control (MPC) is among the most popular control techniques and has been generally adopted by both academic and industrial control communities [1], [2]. It provides a high degree of flexibility, for both performance optimization and constraint handling, as well as an effective way of negotiating the trade-off between computational complexity and cost-function (sub)optimality [1], [3].

Models describing real systems rely on approximations and rarely describe the underlying dynamics of the system to their full extent. This issue is well-known [4] and has given rise to avenues of research on robust and stochastic MPC [5]. *Tube-based MPC*, a practical implementation of the former, tackles model uncertainties and exogenous disturbances by employing a sequence of sets ensuring that all future trajectories of the system will be contained within (see [6]).

To obtain a numerically tractable optimization problem, parameterizations of the sets employed in the tube's definition must be used. The simplest one is called *rigid tube MPC* and it employs fixed size set translations to construct the tube [7]. Scaling the sets produces the so-called *homothetic tube MPC* approaches [8]. Next, in the *parameterized tube MPC* approach, the tube's cross-sections are parameterized via convex hulls described by a finite number of points [9], resulting in a quadratic increase in the number of decision variables w.r.t. the prediction horizon. Another idea is to employ a fixed number of half-spaces in the set description, via an elasticity parameter [10], [11] that controls each half-space's offset, thus, the *elastic tube* moniker. The main benefits of the homothetic and elastic approaches are the enlarged domain of attraction and improved performance.

The sets composing the tube are often polyhedral which negatively affects the MPC problem's size and implementation, due to the complexity of the set description. Ellipsoidal sets [12] are an alternative, but they are relatively conservative in representation and lead to quadratic constraints.

The main idea in the present work is to consider zonotopes [13], which offer an excellent balance between the flexibility of the representation and scalability. Recent works have recognized their potential and embedded them in applications ranging from set estimation [14] to fault detection and isolation [15] and tube MPC constructions [16], [17], [18], [19]. The latest three works use scaled zonotopes [20], [21] to characterize the tube profile, with the key differences from [8], [11] that the scaling factors remain constant along the prediction horizon. Noteworthy, the uncertainty sets in [17], [18], [19] are adjustable. The scaling of zonotope generators is also used to optimize the size of Robust Positive Invariant (RPI) sets [22]. Other approaches aim to reduce the tube's complexity by particular choices of the feedback laws [23].

The main contribution of the present work lies in considering zonotopes, whose generators are independently scaled along the prediction horizon, to implement an elastic tube parameterization with reduced computational complexity through linear set containment conditions. Proposition 3 handles the zonotopic case, while Proposition 2 provides a link to the polyhedral case. The approach improves the existing state-of-the-art methods for tube computation and it is validated on a system with parameterizable size (impractical to handle at higher dimensions through the standard polyhedral variants).

This letter is organized as follows. Section II provides the preliminaries on set operations and zonotopes. The background required for tube MPC along with the computational difficulties associated with this approach are presented in

Manuscript received 4 March 2024; revised 7 May 2024; accepted 24 May 2024. Date of publication 31 May 2024; date of current version 25 June 2024. This work was supported in part by the Ministry of Research, Innovation and Digitization, CCCDI—UEFISCDI within PNCDI III under Project PN-III-P2-2.1-PED-2021-1626, and in part by the RTE Chair at CentraleSupelec. Recommended by Senior Editor L. Zhang. *(Corresponding author: Florin Stoican.)*

Sabin Diaconescu, Florin Stoican, and Bogdan D. Ciubotaru are with the Department of Automatic Control and Systems Engineering, National University of Science and Technology Politehnica Bucharest, 060042 Bucharest, Romania (e-mail: sabin.diaconescu@stud.acs.upb.ro; florin.stoican@upb.ro; bogdan.ciubotaru@upb.ro).

Sorin Olaru is with the Laboratory of Signals and Systems, Univ. Paris-Sud-CentraleSupelec-CNRS, Université Paris Saclay, 91190 Paris, France (e-mail: sorin.olaru@l2s.centralesupelec.fr).

Digital Object Identifier 10.1109/LCSYS.2024.3408047

© 2024 The Authors. This work is licensed under a Creative Commons Attribution 4.0 License.
For more information, see https://creativecommons.org/licenses/by/4.0/

Section III. Section IV provides extensions for the polyhedral variants of tube MPC and addresses the scaled zonotopic tube parameterization facilitating reduced-complexity elastic tube MPC implementations. Section V illustrates a practical application of these techniques in the context of a system with parameterizable size. Section VI summarizes this letter.

Notation: The set of integers residing in intervals $[x_1, x_2] \subset \mathbb{R}$ are denoted by $\mathcal{I}_{[x_1,x_2]}$. If $x_2 = \infty$, the shortcut $\mathcal{I}_{\geq x_1} = \mathcal{I}_{[x_1,\infty]}$ will be used. The term $\mathbf{1}_n$ denotes a vector of ones of length n. For two sets $P, Q \subset \mathbb{R}^n$, $P \oplus Q = \{p + q : \forall p \in P, \forall q \in Q\}$ denotes their Minkowski sum and $P \ominus Q = \{p \in P : \{p\} \oplus Q \subseteq P\}$ denotes their Pontryagin difference. The term $x_{m:n}$ denotes the sequence $\{x_m, \dots, x_n\}$ for some $m, n \in \mathcal{I}_{\geq 0}$. The notation X_i and $X_i^\top$ denote the i-th column and the i-th row of a matrix X, respectively. The symbol $\perp$ denotes orthogonality between two vectors.

II. Preliminaries

Polyhedral sets have a dual representation [13]:

1) half-space description, given by

$$X = \{x \in \mathbb{R}^n : F^\top x \leq \theta\}, \tag{1}$$

where $F \in \mathbb{R}^{n\times q}$ and $\theta \in \mathbb{R}^q$, with q denoting the number of constraints (the "half-spaces");

2) vertex description, given by

$$X = \{x \in \mathbb{R}^n : x = V\alpha,\ \alpha^\top \mathbf{1}_\nu = 1,\ \alpha \in \mathbb{R}^\nu_{\geq 0}\}, \tag{2}$$

where $V \in \mathbb{R}^{n\times\nu}$ gathers as its columns the vertices used in the convex sum description.

This dual representation is one of the reasons for the pervasiveness of polyhedral sets in control applications. In particular, for two sets $X, Y \subset \mathbb{R}^n$, given in half-space (1) and vertex (2) forms, the inclusion $X \subseteq Y$ is equivalent with

$$F_j^\top V_i \leq \theta_j, \quad j \in \mathcal{I}_{[1,q]},\ i \in \mathcal{I}_{[1,\nu]}. \tag{3}$$

A zonotope [13] is a centrally symmetric polytope which can be described as a Minkowski sum of line segments. In its *generator representation*, it is given by

$$Z = \langle c, G\rangle = \{x \in \mathbb{R}^n : x = c + G\xi,\ \|\xi\|_\infty \leq 1\}, \tag{4}$$

where $c \in \mathbb{R}^n$ denotes its *center* and $G \in \mathbb{R}^{n\times D}$ its *generator matrix*. The zonotopes are [13]:

1) closed under affine transformations

$$r \oplus R\langle c, G\rangle = \langle r + Rc, RG\rangle, \tag{5}$$

for any pair r, R of admissible dimensions;

2) closed under Minkowski sum

$$\langle c_1, G_1\rangle \oplus \langle c_2, G_2\rangle = \langle c_1 + c_2, \begin{bmatrix} G_1 & G_2\end{bmatrix}\rangle; \tag{6}$$

3) symmetric: $-\langle c, G\rangle = \langle -c, G\rangle$, up to their center.

A natural extension is the notion of scaled zonotope [20], [21] obtained by denoting $G = G\Delta$, where $\Delta = \mathrm{diag}(\boldsymbol{\delta})$. The rationale for this construction is that parameter $\boldsymbol{\delta} \in \mathbb{R}^D_{\geq 0}$ allows to define an "elastic" boundary for the set but it retains enough structure to keep its description 'simple'.

The process of checking the inclusion of Z in (4) or of its scaled counterpart $Z(c, \boldsymbol{\delta}) = \langle c, G\Delta\rangle$ into X is given by the necessary and sufficient condition [24]

$$\langle c, G\Delta\rangle \subseteq X \Leftrightarrow$$
$$F_i^\top c + \sum_{j=1}^{D} \left|F_i^\top G_j\right| \delta_j \leq \theta_i,\ i \in \mathcal{I}_{[1,q]}. \tag{7}$$

Note that the parameter $\boldsymbol{\delta}$ propagates linearly through the above inclusion and that the idea is equivalent to checking the intersection between a zonotope and a half-space [22].

III. Robust MPC Background

Consider the linear time-invariant (LTI) system

$$x_{k+1} = Ax_k + Bu_k + \omega_k \tag{8}$$

where $x_k, x_{k+1} \in \mathcal{X} \subset \mathbb{R}^n$ denote the current and successor state, $u_k \in \mathcal{U} \subset \mathbb{R}^m$ the control input, and $\omega_k \in \mathcal{W} \subset \mathbb{R}^{m_\omega}$ the exogenous disturbance; the matrices $A \in \mathbb{R}^{n\times n}$, $B \in \mathbb{R}^{n\times m}$ are the known state and input matrices, while $\mathcal{U}$, $\mathcal{X}$ and $\mathcal{W}$ denote the sets bounding their associated signals. For the input sequence $\mathbf{u}_N = \{u_0, u_1, \dots, u_{N-1}\}$, the trajectories of (8), with the initial state $x_0 \in \mathcal{X}_0$, lie in the *feedforward reachable set* sequence

$$\begin{aligned}\mathcal{R}_{k+1}(x_0, \mathbf{u}_k) = \{&Ax_k + Bu_k + \omega_k,\\ &x_k \in \mathcal{R}_k(x_0, \mathbf{u}_{k-1}),\ \omega_k \in \mathcal{W}\}\end{aligned} \tag{9}$$

for $k \in \mathcal{I}_{[0,N-1]}$, $\mathcal{R}_0(x_0, \emptyset) = \mathcal{X}_0$, and $\mathbf{u}_k$ an admissible sequence of inputs.

Owing to the superposition property of linear dynamics, (8) can be decomposed into its 'nominal' dynamics,

$$\bar{x}_{k+1} = A\bar{x}_k + B\bar{u}_k, \tag{10}$$

and its state tracking error dynamics ($z_k = x_k - \bar{x}_k$),

$$z_{k+1} = Az_k + Bv_k + \omega_k, \tag{11}$$

linked through the control action $u_k = \bar{u}_k + v_k$, whose components may be seen as a combination of feedforward action ($\bar{u}_k$), which steers (10), and feedback action (v_k), which ensures the stability and disturbance rejection of (11). This allows to recast the set recurrence, in the parlance of [25], [26], into nominal and disturbance-affected components $\mathcal{R}_k(x_0, \mathbf{u}_k) = \{\bar{x}_k\} \oplus \mathcal{R}_k(z_0, \mathbf{v}_k)$.

To do so, consider the bounding sets $\Omega_k, \mathcal{V}_k$ verifying set inclusions

$$z_k \in \mathcal{R}_k(z_0, \mathbf{v}_k) \subseteq \Omega_k, \quad v_k \in \mathcal{V}_k, \quad \forall k \in \mathcal{I}_{[0,N]}. \tag{12}$$

Then, the tube MPC problem is given by [27]

$$\bar{\mathbf{u}}_N^\star = \arg\min_{\bar{\mathbf{u}}_N} \bar{x}_N^\top P\bar{x}_N + \sum_{k=0}^{N-1}\left(\bar{x}_k^\top Q\bar{x}_k + \bar{u}_k^\top R\bar{u}_k\right), \tag{13a}$$
$$\text{s.t. } \bar{x}_{k+1} = A\bar{x}_k + B\bar{u}_k,\ k \in \mathcal{I}_{[0,N-1]}, \tag{13b}$$
$$\{\bar{x}_k\} \oplus \Omega_k \subseteq \mathcal{X},\ k \in \mathcal{I}_{[0,N-1]}, \tag{13c}$$
$$\{\bar{u}_k\} \oplus \mathcal{V}_k \subseteq \mathcal{U},\ k \in \mathcal{I}_{[0,N-1]}, \tag{13d}$$
$$\{\bar{x}_N\} \oplus \Omega_N \subseteq \mathcal{T}. \tag{13e}$$

Along a prediction horizon of length N, the nominal state is updated in (13b), stage state and inputs are bounded by the tightened constraints (13c) and (13d), and the terminal state is bounded by a tightened terminal set (13e), with the standard control invariant properties. The cost is quadratic and it is defined in (13a) by matrices $Q \in \mathbb{R}^{n\times n}$, $R \in \mathbb{R}^{m\times m}$ and $P \in \mathbb{R}^{n\times n}$, which are positive (semi-)definite and symmetric, i.e., $Q = Q^\top \succeq 0$, $R = R^\top \succ 0$, $P = P^\top \succeq 0$. The term u_k, applied to the system (8), is obtained by selecting the first element of the optimal control sequence $\bar{\mathbf{u}}_N^\star \in \mathbb{R}^{Nm}$, to which the feedback term v_k is appended.

The linchpin of the formulation (13) is the nature and the computational aspect of the sets $\Omega_k, \mathcal{V}_k$ from (12), which tighten the constraints (13c)–(13e). At first glance, this allows the definition of $\Omega_k = \mathcal{R}_k(\mathcal{Z}_0, \mathbf{v}_k)$ as the feedforward reachable set of dynamics (11). Unfortunately, the complexity of Ω_k quickly becomes unmanageable and various over-approximations have to be used. The choices range from the simple initial rigid tube approach of [7] to the more recent homothetic [8] and elastic [10], [11] tube ones, which allow changes in the tube's profile along the prediction horizon. In any case, the admissibility condition that has to be verified becomes

$$\{Az_k + B\pi(z_k) : z_k \in \Omega_k\} \oplus \mathcal{W} \subseteq \Omega_{k+1}, \tag{14}$$

with $v_k = \pi(z_k)$, an a priori fixed feedback control policy. When, $v_k = Kz_k$, with K a static feedback gain ensuring closed loop stability for dynamics (11), (14) becomes

$$(A + BK)\Omega_k \oplus \mathcal{W} \subseteq \Omega_{k+1}, \tag{15}$$

and, furthermore, $\mathcal{V}_k = \{\pi(z_k) : z_k \in \Omega_k\} = K\Omega_k$.

Some of the aforementioned tube MPC variants consider either polyhedral sets, with clear limitations on the complexity and the fragility of their ancillary algorithms [13], or ellipsoidal sets, which have robust algorithms but are conservative w.r.t. the set description. Our goal is to adapt the pioneering and state of the art work of the elastic tube parameterization approach [11] to the scaled zonotopic case. The next section paves the way.

IV. Robust MPC With Scaled Zonotopic Sets

This section recalls the polyhedral approach from [11] and uses it to introduce the elastic zonotopic approach for which further constructive and computational aspects are presented.

A. Extensions for the Polyhedral Elastic Tube

Let us consider polyhedral sets $P, Q \subset \mathbb{R}^n$ given in half-space form (1) and a vector $\bar{d} \in \mathbb{R}^n$. Classically, inclusion $P \oplus \{\bar{d}\} \subseteq Q$ holds iff

$$\max_{x\in P} F_Q x + F_Q \bar{d} \le \theta_Q \tag{16}$$

holds element-wise. Unfortunately, checking (16) requires the vertex description of the inner polytope P. Among many others, [28] makes use of a necessary and sufficient condition which involves only the half-space representation of the polytopes, as illustrated in the following lemma.

Lemma 1: Inclusion $P \oplus \{\bar{d}\} \subseteq Q$ holds iff it exists $H \in \mathbb{R}_{\ge 0}^{n_P \times n_Q}$ which verifies

$$H \ge 0, \quad HF_P = F_Q, \quad H\theta_P + F_Q\bar{d} \le \theta_Q. \tag{17}$$

Remark 1: Note that as long as P and Q are fixed, relations (17) are linear in matrix H.

For further use we recall next a slight variation of the polytopic elastic tube MPC presented in [11].

Proposition 1: Considering the parameterized polyhedral set

$$S(\mathbf{a}) = \{x \in \mathbb{R}^n : F_S x \le \mathbf{a}\} \tag{18}$$

with $\mathbf{a} \in \mathbb{R}_{\ge 0}^{q_S}$, and denoting $\Omega_k = S(\mathbf{a}_k)$, $\mathcal{V}_k = KS(\mathbf{a}_k)$, the MPC problem (13) becomes

$$\bar{\mathbf{u}}_N^\star = \arg\min_{\bar{\mathbf{u}}_N, \mathbf{a}_1,\dots,\mathbf{a}_N} \bar{x}_N^\top P\bar{x}_N + \sum_{k=0}^{N-1}\Big(\bar{x}_k^\top Q\bar{x}_k + \bar{u}_k^\top R\bar{u}_k\Big), \tag{19a}$$

$$\begin{aligned}
\text{s.t. } \bar{x}_{k+1} &= A\bar{x}_k + B\bar{u}_k,\ k \in \mathcal{I}_{[0,N-1]}, && (19b)\\
H_S &\ge 0,\ H_S F_S(A + BK) = F_S, && (19c)\\
H_S\mathbf{a}_k + \bar{\omega} &\le \mathbf{a}_{k+1},\ k \in \mathcal{I}_{[0,N-1]}, && (19d)\\
H_X &\ge 0,\ H_X F_S = F_X, && (19e)\\
H_X\mathbf{a}_k + F_X\bar{x}_k &\le \theta_X,\ k \in \mathcal{I}_{[0,N-1]}, && (19f)\\
H_U &\ge 0,\ H_U F_S = F_U K, && (19g)\\
H_U\mathbf{a}_k + F_U\bar{u}_k &\le \theta_U,\ k \in \mathcal{I}_{[0,N-1]}, && (19h)\\
H_T &\ge 0,\ H_T F_S = F_U, && (19i)\\
H_T\mathbf{a}_k + F_T\bar{x}_N &\le \theta_T, && (19j)
\end{aligned}$$

with shorthand $\bar{\omega} = \max_{\omega\in\mathcal{W}} F_S\omega$.

Proof: To derive (19), we need to express, via Lemma 1, the set inclusions from (13) and (15), modified to use the elastic sets $S(\mathbf{a}_k)$ defined in (18). In the case of (15), and noticing $\Omega_k = S(\mathbf{a}_k)$, the set inclusion becomes $(A + BK)S(\mathbf{a}_k) \oplus \mathcal{W} \subseteq S(\mathbf{a}_{k+1})$, which, via Lemma 1, is equivalent with checking (19c)–(19d). The set inclusions (13c) and (13e) can be reformulated similarly and correspond to the group of constraints (19e)–(19h) and (19i)–(19j). ∎

Remark 2: While matrices $H_{\{S,X,U,T\}}$ and vector $\bar{\omega}$ may be part of the optimization problem, in the case of (19) they are computed before the first call of the MPC problem. The caveat is that $H_{\{S,X,U,T\}}$ matrices are not unique and a priori fixing them may lead to a sub-optimal solution. A simpler formulation is presented in [11] but it is mainly required because the gain K is allowed to vary along the prediction horizon. Here, a static gain has been chosen to carry computations offline and the only additional variables introduced in the original MPC problem are the scaling factors $\{\mathbf{a}_k\}_{k=1:N}$.

Remark 3: The introduction of scaling factors in (19) may lead to an infeasible problem, as (19d) imposes a relation between successive values $\mathbf{a}_k, \mathbf{a}_{k+1}$ which may make infeasible the constraints (19f), (19h) or (19j).

Imposing a particular structure on the elements of the scaling vector $\mathbf{a}_k$ allows to describe either the homothetic case, where $\mathbf{a}_k = a_k \cdot \mathbf{1}$, with $a_k \in \mathbb{R}_{\ge 0}$, or the elastic case, where each element of $\mathbf{a}_k$ is an independent variable.

B. The Scaled Zonotope Variation

Recalling the definition of a scaled zonotope, one can use it to replace (18) in Section IV-A by

$$Z(c, \boldsymbol{\delta}) = \langle c, G\Delta\rangle \tag{20}$$

with $G \in \mathbb{R}^{n\times D}$, $\boldsymbol{\delta} \in \mathbb{R}_{\ge 0}^D$. The ultimate goal is to work directly with the generator representation (4). In order to do so, the polyhedral representation of the zonotopic set is used to show that (20) maybe be brought into the form of (18).

Proposition 2: Any scaled zonotope (20) may be equivalently written as a polyhedral set (18) with the scaling factor

$$\boldsymbol{a} = \begin{bmatrix} F^\top c \\ -F^\top c \end{bmatrix} + \begin{bmatrix} \Theta^\top \\ \Theta^\top \end{bmatrix}\boldsymbol{\delta}, \tag{21}$$

where each pair $(F_i, \Theta_i) \in \mathbb{R}^n \times \mathbb{R}^D_{\geq 0}$, $i \in \mathcal{I}_{[1,q]}$, comes from

$$F_i \text{ verifying } F_i \perp G_{j_\ell}, \forall j_\ell \in \{j_1 \dots j_{n-1}\}, \tag{22a}$$
$$\Theta_i^\top \boldsymbol{\delta} = \sum_{j_\ell \notin \{j_1 \dots j_{n-1}\}} \left| F_i^\top G_{j_\ell} \right| \delta_{j_\ell}, \tag{22b}$$

with the j_ℓ-th entry of $\Theta_i \in \mathbb{R}^D_{\geq 0}$ equal to $|F_i^\top G_{j_\ell}|$ if $j_\ell \notin \{j_1 \dots j_{n-1}\}$ and 0, otherwise.

Proof: For the scaled zonotope (20), each sequence of $n-1$ generators $1 \leq j_1 < \dots < j_{n-1} \leq D$, has a corresponding pair $(F_i, \Theta_i^\top \boldsymbol{\delta}) \in \mathbb{R}^n \times \mathbb{R}$ [29]. Adding the center c, we arrive at the half-space representation

$$\langle c, G\Delta \rangle = \bigcap_{j \in \mathcal{I}_{[1,D]}} \{x \in \mathbb{R}^n : \left| F_i^\top (x - c) \right| \leq \Theta_i^\top \boldsymbol{\delta}\}, i \in \mathcal{I}_{[1,q]},$$
$$= \left\{ x \in \mathbb{R}^n : \begin{bmatrix} F^\top \\ -F^\top \end{bmatrix} x \leq \begin{bmatrix} F^\top c \\ -F^\top c \end{bmatrix} + \begin{bmatrix} \Theta^\top \\ \Theta^\top \end{bmatrix} \boldsymbol{\delta} \right\}, \tag{23}$$

which directly leads to (21). ∎

The result may be used for any of the set containment constraints from (19), whenever the sets considered are scaled zonotopes (20), the elastic term is replaced with (21).

Naturally, one would like to avoid altogether the half-space representation of $Z(c, \boldsymbol{\delta})$ when enforcing the set inclusions (13c)–(13e) and (15). The set containment conditions which involve zonotopic sets are firstly recalled (see [17], [28]).

Lemma 2: For a pair of zonotopes $Z_{\{1,2\}} = \langle c_{\{1,2\}}, G_{\{1,2\}} \rangle$, with $c_{\{1,2\}} \in \mathbb{R}^n$, $G_{\{1,2\}} \in \mathbb{R}^{n \times D_{\{1,2\}}}$, and a polytope $P = \{x : F_P x \leq \theta_P\}$, with $F_P \in \mathbb{R}^{q_P \times d}$, $\theta_P \in \mathbb{R}^{q_P}$, we have that:

1) a sufficient condition to verify the inclusion $Z_1 \subseteq Z_2$ is the existence of Γ, γ s.t.

$$G_1 = G_2 \Gamma, \; c_1 - c_2 = G_2 \gamma, \; |\Gamma| \mathbf{1}_{D_1} + |\gamma| \leq \mathbf{1}_{D_1}; \tag{24}$$

2) a necessary and sufficient condition to verify the inclusion $Z_1 \subseteq P$ is

$$F_P c_1 + |F_P G_1| \mathbf{1}_{D_1} \leq \theta_P. \tag{25}$$

Next, set inclusion conditions are provided for the case with time-varying scaling factors, extending the result from [17, Th. 4], which handles constant scaling factors.

Proposition 3: For the scaled zonotope $Z(c_k, \boldsymbol{\delta}_k)$, taking $\bar{x}_k \in Z(c_k, \boldsymbol{\delta}_k)$ and $\bar{u}_k \in KZ(c_k, \boldsymbol{\delta}_k)$, set inclusions (13c)–(13e) and (15) are verified by the sufficient conditions

$$F_X(c_k + \bar{x}_k) + |F_X G| \boldsymbol{\delta}_k \leq \theta_X, \tag{26a}$$
$$F_U(Kc_k + \bar{u}_k) + |F_U K G| \boldsymbol{\delta}_k \leq \theta_U, \tag{26b}$$
$$F_T(c_N + \bar{x}_N) + |F_T G| \boldsymbol{\delta}_N \leq \theta_T, \tag{26c}$$
$$(c_k + c_\omega) - c_{k+1} = G\gamma_k, \; |\gamma_k| + |\Gamma|(\boldsymbol{\delta}_k + \boldsymbol{\delta}_\omega) \leq \boldsymbol{\delta}_{k+1}, \tag{26d}$$

for all $k \in \mathcal{I}_{[0,N-1]}$ and with $\Gamma \in \mathbb{R}^{D \times D}$ verifying $A_K G = G\Gamma$, $A_K = A + BK$ and where $\mathcal{W} \subseteq \langle c_w, A_k G \Delta_\omega \rangle$, with $\Delta_\omega = \text{diag}(\boldsymbol{\delta}_\omega)$.

Proof: Using $Z(c_k, \boldsymbol{\delta}_k) = \langle c_k, G\Delta_k \rangle$, defined in (20), inclusions (13c)–(13e) and (15) become

$$\langle c_k + \bar{x}_k, G\Delta_k \rangle \subseteq \mathcal{X}, \tag{27a}$$
$$\langle Kc_k + \bar{u}_k, KG\Delta_k \rangle \subseteq \mathcal{U}, \tag{27b}$$
$$\langle c_N + \bar{x}_N, G\Delta_N \rangle \subseteq \mathcal{T}, \tag{27c}$$
$$\langle c_k, A_K G \Delta_k \rangle \oplus \mathcal{W} \subseteq \langle c_{k+1}, G\Delta_{k+1} \rangle, \tag{27d}$$

for all $k \in \mathcal{I}_{[0,N-1]}$. Inclusions (27a)–(27b) fall under (25) and may be immediately put into the form (26a)–(26c) once we note that $|\Delta_k| = \Delta_k$ and that $\Delta_k \mathbf{1}_D = \boldsymbol{\delta}_k$. In the case of (27d), some preliminaries are needed. First, using $\mathcal{W} \subseteq \langle c_\omega, A_K G \Delta_\omega \rangle$, we upper bound the left-hand side of (27d) as $\langle c_k + c_\omega, A_K G(\Delta_k + \Delta_\omega) \rangle$, which brings it now into the form of (24). Second, recall $A_K G = G\Gamma$ assumed in the initial statement and take γ_k which verifies $(c_k + c_\omega) - c_{k+1} = G\gamma_k$. These relations may be put into the form

$$A_K G(\Delta_k + \Delta_\omega) = G\Delta_{k+1} \cdot \Delta_{k+1}^{-1} \Gamma (\Delta_k + \Delta_\omega), \tag{28a}$$
$$(c_k + c_\omega) - c_{k+1} = G\Delta_{k+1} \cdot \Delta_{k+1}^{-1} \gamma_k. \tag{28b}$$

Introducing $\Gamma = \Delta_{k+1}^{-1} \Gamma (\Delta_k + \Delta_\omega)$ and $\gamma = \Delta_{k+1}^{-1} \gamma_k$ in (24), we obtain $|\Delta_{k+1}^{-1} \gamma_k| + |\Delta_{k+1}^{-1} \Gamma (\Delta_k + \Delta_\omega)| \mathbf{1}_D \leq \mathbf{1}_D$ as a sufficiency test for inclusion (27d). Left multiplying with the element-wise positive Δ_{k+1} brings us to $|\gamma_k| + |\Gamma|(\Delta_k + \Delta_\omega)\mathbf{1}_D \leq \Delta_{k+1} \mathbf{1}_D$ and noting that $\Delta_{\{k,k+1,\omega\}} \mathbf{1}_D = \boldsymbol{\delta}_{\{k,k+1,\omega\}}$ leads to (26d), thus concluding the proof. ∎

Centering the state and input tubes (taking $c_k = 0$) in the nominal values $\bar{x}_k, \bar{u}_k$ reduces the complexity, since $\bar{x}_k$ and $\bar{u}_k$ are already within the sets and it is no longer necessary to explicitly constrain them.

The recursive feasibility and stability topics in the context of tube MPC are described in more detail in [7], [11], [17], [30]. Since the presented approach is using a different tube parameterization all the robustness and stability guarantees provided by the elastic approach [11] are being preserved.

Remark 4: Pre-computing Γ makes all inequalities in (26) linear and easy to embed into the larger MPC problem. For further use, we take it as the result of the following minimization problem, similar to [11, Sec III.A],

$$\Gamma = \arg\min_{X, \gamma} \|X\|_F$$
$$\text{s.t. } c_\omega = G\gamma, A_K G = GX, |\gamma| + |X| \mathbf{1}_D \leq \mathbf{1}_D. \tag{29}$$

The apparent non-linearity induced by the module disappears if we reformulate (26d) as

$$|\gamma_k| \leq \boldsymbol{\delta}_{k+1} - |\Gamma|(\boldsymbol{\delta}_k + \boldsymbol{\delta}_\omega), \tag{30}$$

and note its equivalence with the inclusion

$$\gamma_k \in \text{CR}_D \cdot (\delta_{k+1} - |\Gamma|(\boldsymbol{\delta}_k + \boldsymbol{\delta}_\omega)), \tag{31}$$

where CR_D denotes the unit cross-polytope from $\mathbb{R}^D$ (the polar set of the hypercube [13]).

Remark 5: Note that the number of inequalities in (23) is significantly smaller when using the generator representation rather than when using the half-space representation.

Remark 6: Proposition 3 reduces to the homothetic case by enforcing all components of the scaling vector to be equal, $\boldsymbol{\delta}_{\{k,\omega\}} = \delta_{\{k,\omega\}} \cdot \mathbf{1}_D$ for $k \in \mathcal{I}_{[0,N-1]}$ in (26).

Since the mRPI is the result of an infinite set recurrence, we provide a zonotopic 'one-step RPI' approximation in the next proposition (extended from [28, Th. 6] and [17, Th. 2]).

The choice of the seed generator matrix G and center c is not unique, but the shape of the set $\langle c, G\rangle$ should be chosen to ensure feasibility of the linear constraints used to enforce the RPI set containment condition for the closed-loop dynamics $x_{k+1} = A_K x_k + \omega$, with $\omega \in \mathcal{W}$.

Proposition 4: Let $\mathcal{W} \subseteq \langle c_0, G_0\rangle$ and construct $\bar{G} = \left[I \; A_K \; \dots \; A_K^s\right] G_0 \in \mathbb{R}^{n\times D}$ for some fixed positive integer s. Then, minimizing the linear program

$$\min_{c,\boldsymbol{\delta},\Gamma_1,\Gamma_2,\boldsymbol{\beta},\boldsymbol{\alpha}_1,\dots,\boldsymbol{\alpha}_D} \quad \mathbf{1}_D^\top \boldsymbol{\delta} \tag{32a}$$

$$\text{s.t.} \quad \boldsymbol{\delta} \geq 0, \tag{32b}$$

$$A_K \bar{G}\cdot \text{diag}(\boldsymbol{\delta}) = \bar{G}\Gamma_1, \quad G_0 = \bar{G}\Gamma_2 \tag{32c}$$

$$(I - A_K)c - c_0 = \bar{G}\boldsymbol{\beta}, \tag{32d}$$

$$\boldsymbol{\alpha}_i \geq 0,\ \mathbf{1}_D^\top \boldsymbol{\alpha}_i \leq \delta_i,\ \forall i \in \mathcal{I}_{[1,D]}, \tag{32e}$$

$$\begin{bmatrix} I & -I\end{bmatrix}\boldsymbol{\alpha}_i = \begin{bmatrix}\Gamma_{1,i} & \Gamma_{2,i} & \beta_i\end{bmatrix}^\top,\ \forall i \in \mathcal{I}_{[1,D]}, \tag{32f}$$

provides the center c and the scaling factor $\boldsymbol{\delta}$ such that the zonotopic set $\langle c, G = \bar{G}\boldsymbol{\delta}\rangle$ is RPI under the dynamics $x_{k+1} = A_K x_k + \omega$, with $\omega \in \mathcal{W}$. Index i in $\Gamma_{1,i}, \Gamma_{2,i}, \beta_i$ denotes the i-th row from matrices Γ_1, Γ_2 and vector $\boldsymbol{\beta}$.

Proof: The proposition builds upon [22, Th. 6], where the inclusion test $|\Gamma_1|\mathbf{1}_D + |\Gamma_2|\mathbf{1}_D + |\boldsymbol{\beta}| \leq \boldsymbol{\delta}$, similar with (24), is replaced with (32e)–(32f), checking the inclusion of a vector inside the cross-polytope, as discussed in Remark 4 and implemented in [31]. ■

V. Simulation and Results

The proposed implementation is illustrated for the double integrator used in [11] and the CSE1 example given in [32]. The optimization problems are solved in MATLAB, using YALMIP [33] and MOSEK [34], on a computer with a 2.1GHz i7 Intel processor with 12 cores and 32GB RAM, while the zonotopic and polyhedral sets are implemented in CORA [29] and MPT3 [35].

A. Double Integrator [11]

We revisit the example from [11] applying our zonotopic constructions in 1 for all three tube variants: rigid from Proposition 4 (···◆···), homothetic from Remark 6 (—▲—), and elastic from Proposition 3 (- -■- -).

In a common MPC setting, $Q = I$, $R = 0.01$, $N = 12$, $\mathcal{X} = [-10, 10] \times [-10, 2]$, $\mathcal{U} = [-1, 1]$, $\mathcal{T} = \{0\}$, $\mathcal{W} = [-0.1, 0.1] \times [-0.1, 0.1]$, all tube variants provide feasible solutions.

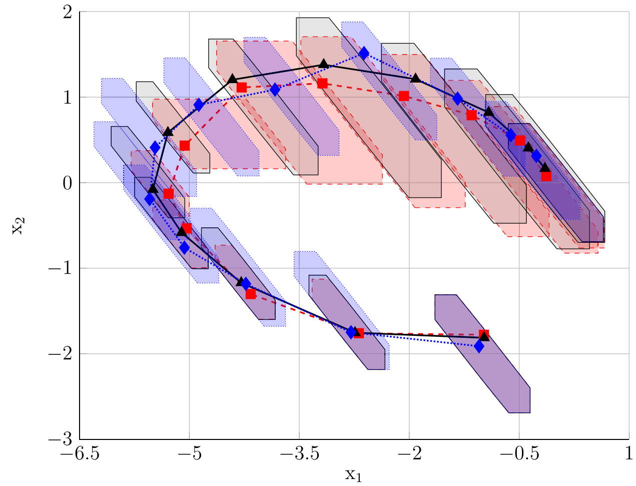

Fig. 1. One finite horizon optimal state sequence.

B. Coupled Spring Experiment - ‘CSE1’ [32]

While helpful for illustration purposes, the double integrator cannot provide sufficient insights for computational effort quantification. To assess the influence of the problem size, we consider the continuous-time ‘CSE’ dynamics, given in *COMPl$_e$ib* [32], which describe a system combining coupled springs, dampers and masses. The mass positions and velocities define the system’s states. Its inputs are the two forces exerted at the ends of the coupled springs chain [32]. The parameter ℓ denotes the number of springs and governs the model’s size (2ℓ), given by

$$\dot{x} = \underbrace{\begin{bmatrix} 0 & I \\ -M_c^{-1}K_c & -M_c^{-1}L_c\end{bmatrix}}_{\mathrm{A}\in\mathbb{R}^{2\ell\times 2\ell}} x + \underbrace{\begin{bmatrix} 0 \\ M_c^{-1}D_c\end{bmatrix}}_{\mathrm{B}\in\mathbb{R}^{2\ell\times 2}} u, \tag{33}$$

where

$$K_c = k\begin{bmatrix} 1 & -1 & \cdots & 0 & 0 \\ -1 & -2 & \ddots & 0 & 0 \\ \vdots & \ddots & \ddots & \ddots & \vdots \\ 0 & 0 & \ddots & -2 & -1 \\ 0 & 0 & \cdots & -1 & 1 \end{bmatrix}, \quad D_c = \begin{bmatrix} 1 & 0 \\ 0 & 0 \\ \vdots & \vdots \\ 0 & 0 \\ 0 & -1\end{bmatrix},$$

and $M_c = \mu I$, $L_c = \delta I$. The parameter values are $\mu = 4$, $\delta = 1$, $k = 1$ and the system is discretized with the forward Euler method for a sampling time of 1 sec. The state and input constraints are $\mathcal{X} = [-1, 1]^{2\ell}$, $\mathcal{U} = [-1, 1]^2$, $\mathcal{W} = [-0.01, 0.01]^{2\ell}$, while the MPC parameters are $Q = I_{2\ell}$, $R = 0.01 I_2$, $N = 25$. Several conclusions can be drawn:

- all tube polyhedral set implementations fail around $\ell \geq 3$, by exceeding a computational time limit, a maximum allowed number of iterations or by not finding a solution, whereas the zonotopic ones work over the entire parameter range considered, until $\ell = 10$;
- clearly the nominal case is the most efficient implementation but it does not provide any robustness guarantees;
- the underlying set containment conditions using zonotopic sets result in linear complexity;
- all tube methods are greatly affected by the choice of the initial set $Z(c, \boldsymbol{\delta}_0 = 1)$; finding an optimal balance between the accuracy of the minimal RPI set approximation and the difficulty of solving the MPC problem is, in the authors’ opinion, still an open question.

VI. Conclusion

The usage of elastically-scaled zonotopes employed in the elastic-tube MPC optimization problem provides significant computational advantages, while reducing the execution time and dimension-related difficulties. The applicability of the procedure is proven on a couple of benchmark models, one of them corresponding to a system with parameterizable size, demonstrating the effectiveness of handling bounded additive disturbances on challenging design frameworks. A comparison between several tube parameterizations and set types along with their associated execution times is given

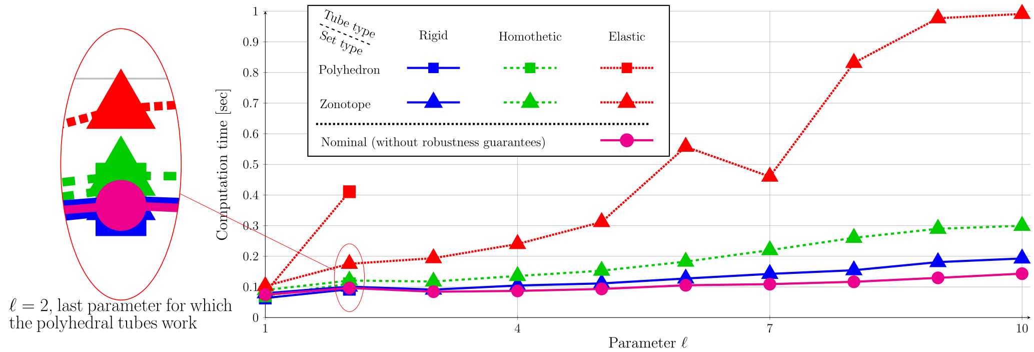

Fig. 2. Comparison of execution times with different tube profiles and set types.

in Fig. 2. Future work will focus on reducing the complexity of the initial RPI set through dynamic controller synthesis.

References

[1] J. Rawlings, D. Mayne, and M. Diehl, *Model Predictive Control: Theory, Computation, and Design*. Santa Barbara, CA, USA: Nob Hill Publ., 2017.

[2] D. Q. Mayne, "Model predictive control: Recent developments and future promise," *Automatica*, vol. 50, no. 12, pp. 2967–2986, 2014.

[3] F. Borrelli, A. Bemporad, and M. Morari, *Predictive Control for Linear and Hybrid Systems*. Cambridge, U.K.: Cambridge Univ. Press, 2017.

[4] M. Morari and J. H. Lee, "Model predictive control: Past, present and future," *Comput. Chem. Eng.*, vol. 23, no. 4, pp. 667–682, 1999.

[5] B. Kouvaritakis and M. Cannon, *Model Predictive Control: Classical, Robust and Stochastic*. Cham, Switzerland: Springer, 2016.

[6] F. Blanchini and S. Miani, *Set-Theoretic Methods in Control*, 2nd ed. Cham, Switzerland: Birkhäuser, 2008.

[7] D. Mayne, M. Seron, and S. Raković, "Robust model predictive control of constrained linear systems with bounded disturbances," *Automatica*, vol. 41, no. 2, pp. 219–224, 2005.

[8] S. V. Raković, B. Kouvaritakis, R. Findeisen, and M. Cannon, "Homothetic tube model predictive control," *Automatica*, vol. 48, no. 8, pp. 1631–1638, 2012.

[9] S. V. Rakovic, B. Kouvaritakis, M. Cannon, C. Panos, and R. Findeisen, "Parameterized tube model predictive control," *IEEE Trans. Autom. Control*, vol. 57, no. 11, pp. 2746–2761, Nov. 2012.

[10] J. Fleming, B. Kouvaritakis, and M. Cannon, "Robust tube MPC for linear systems with multiplicative uncertainty," *IEEE Trans. Autom. Control*, vol. 60, no. 4, pp. 1087–1092, Apr. 2015.

[11] S. V. Raković, W. S. Levine, and B. Açikmese, "Elastic tube model predictive control," in *Proc. Amer. Control Conf.*, 2016, pp. 3594–3599.

[12] A. Parsi, A. Iannelli, and R. S. Smith, "Scalable tube model predictive control of uncertain linear systems using ellipsoidal sets," 2022, *arXiv:2204.02134*.

[13] K. Fukuda, "Polyhedral computation," Lecture Notes, Dept. Math., Inst. Theor. Comput. Sci., ETH Zurich, Switzerland, 2020.

[14] B. S. Rego, G. V. Raffo, J. K. Scott, and D. M. Raimondo, "Guaranteed methods based on constrained zonotopes for set-valued state estimation of nonlinear discrete-time systems," *Automatica*, vol. 111, Jan. 2020, Art. no. 108614.

[15] D. M. Raimondo, G. R. Marseglia, R. D. Braatz, and J. K. Scott, "Closed-loop input design for guaranteed fault diagnosis using set-valued observers," *Automatica*, vol. 74, pp. 107–117, Dec. 2016.

[16] R. Andrade, J. E. Normey-Rico, and G. V. Raffo, "Tube-based model predictive control based on constrained zonotopes," *IEEE Access*, vol. 12, pp. 50100–50113, 2024.

[17] V. Raghuraman and J. P. Koeln, "Tube-based robust MPC with adjustable uncertainty sets using zonotopes," in *Proc. Amer. Control Conf. (ACC)*, 2021, pp. 462–469.

[18] W. Wang and J. P. Koeln, "Tube-based robust MPC for two-timescale systems using reduced-order models," *IEEE Control Syst. Lett.*, vol. 7, pp. 799–804, 2023.

[19] V. Raghuraman and J. P. Koeln, "Hierarchical MPC for coupled subsystems using adjustable tubes," *Automatica*, vol. 143, Sep. 2022, Art. no. 110435.

[20] D. Ioan, S. Olaru, S.-I. Niculescu, I. Prodan, and F. Stoican, "Navigation in a multi-obstacle environment. from partition of the space to a zonotopic-based MPC," in *Proc. 18th Eur. Control Conf. (ECC)*, 2019, pp. 1772–1777.

[21] L. Yang and N. Ozay, "Scalable zonotopic under-approximation of backward reachable sets for uncertain linear systems," *IEEE Control Syst. Lett.*, vol. 6, pp. 1555–1560, 2021.

[22] V. Raghuraman and J. P. Koeln, "Set operations and order reductions for constrained zonotopes," *Automatica*, vol. 139, May 2022, Art. no. 110204.

[23] A. Richards and J. How, "Robust stable model predictive control with constraint tightening," in *Proc. Amer. Control Conf.*, 2006, pp. 1557–1562.

[24] A. Girard, "Reachability of uncertain linear systems using Zonotopes," in *Proc. Int. Workshop Hybrid Syst., Comput. Control*, 2005, pp. 291–305.

[25] P. J. Goulart, E. C. Kerrigan, and J. M. Maciejowski, "Optimization over state feedback policies for robust control with constraints," *Automatica*, vol. 42, no. 4, pp. 523–533, 2006.

[26] S. Raković, E. Kerrigan, D. Mayne, and K. Kouramas, "Optimized robust control invariance for linear discrete-time systems: Theoretical foundations," *Automatica*, vol. 43, no. 5, pp. 831–841, 2007.

[27] B. Houska and M. E. Villanueva, "Robust optimization for MPC," in *Handbook of Model Predictive Control*, S. V. Raković and W. S. Levine, Eds. Cham, Switzerland: Springer, 2019, pp. 413–443.

[28] S. Sadraddini and R. Tedrake, "Linear encodings for polytope containment problems," in *Proc. IEEE 58th Conf. Decis. Control (CDC)*, 2019, pp. 4367–4372.

[29] M. Althoff, "An introduction to CORA 2015," in *Proc. 1st 2nd Workshop Appl. Verificat. Continu. Hybrid Syst.*, 2015, pp. 120–151.

[30] D. Mayne, J. Rawlings, C. Rao, and P. Scokaert, "Constrained model predictive control: Stability and optimality," *Automatica*, vol. 36, no. 6, pp. 789–814, 2000.

[31] B. Gheorghe, F. Stoican, and I. Prodan, "On the complexity of computing the maximal positive invariant set," in *Proc. Eur. Control Conf.*, 2024, to be published. [Online]. Available: https://shorturl.at/uCFJX

[32] F. Leibfritz, *COMPleib: COnstrained Matrix–Optimization Problem Library–A Collection of Test Examples for Nonlinear Semidefinite Programs, Control System Design and Related Problems*, Univ. Trier, Trier, Germany, 2006.

[33] J. Löfberg, "Automatic robust convex programming," *Optim. Methods Softw.*, vol. 27, no. 1, pp. 115–129, 2012.

[34] (MOSEK ApS, Copenhagen, Denmark). *The MOSEK Optimization Toolbox for MATLAB Manual, Version 10.1*. 2024. [Online]. Available: http://docs.mosek.com/latest/toolbox/index.html

[35] M. Herceg, M. Kvasnica, C. Jones, and M. Morari, "Multi-parametric toolbox 3.0," in *Proc. Eur. Control Conf.*, Zürich, Switzerland, 2013, pp. 502–510.